



This is a repository copy of *Well-defined networks from DGEFB - the importance of regioisomerism in epoxy resin networks*.

White Rose Research Online URL for this paper:
<https://eprints.whiterose.ac.uk/150429/>

Version: Published Version

Article:

Knox, S.T., Wright, A., Cameron, C. et al. (1 more author) (2019) Well-defined networks from DGEFB - the importance of regioisomerism in epoxy resin networks. *Macromolecules*, 52 (18). pp. 6861-6867. ISSN 0024-9297

<https://doi.org/10.1021/acs.macromol.9b01441>

Reuse

This article is distributed under the terms of the Creative Commons Attribution (CC BY) licence. This licence allows you to distribute, remix, tweak, and build upon the work, even commercially, as long as you credit the authors for the original work. More information and the full terms of the licence here:
<https://creativecommons.org/licenses/>

Takedown

If you consider content in White Rose Research Online to be in breach of UK law, please notify us by emailing eprints@whiterose.ac.uk including the URL of the record and the reason for the withdrawal request.



eprints@whiterose.ac.uk
<https://eprints.whiterose.ac.uk/>

Well-Defined Networks from DGEBF—The Importance of Regioisomerism in Epoxy Resin Networks

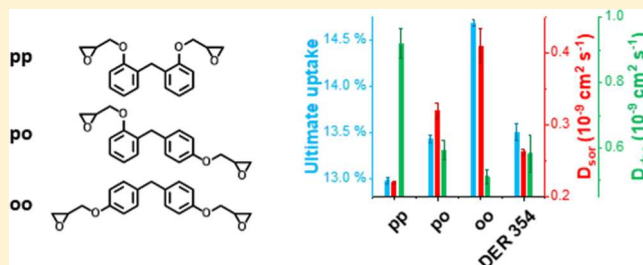
Stephen T. Knox,^{*,†,§} Anthony Wright,[‡] Colin Cameron,[‡] and John Patrick Anthony Fairclough[†]

[†]Department of Mechanical Engineering, University of Sheffield, Sheffield S1 4BJ, U.K.

[‡]AkzoNobel, International Paint Limited, Stoneygate Lane, Gateshead NE10 0JY, U.K.

Supporting Information

ABSTRACT: The previously ignored or unreported impact of regioisomerism within diglycidyl ether of bisphenol F (DGEBF) on its network properties is presented. Routes to the isomers of DGEBF were explored: high-performance liquid chromatography showed good separation of the three isomers [*para*–*para*-DGEBF (ppDGEBF), *para*–*ortho*-DGEBF (poDGEBF), and *ortho*–*ortho*-DGEBF (ooDGEBF)] with small yields; column chromatography gave good separation of pp- + po- from oo-DGEBF but pp-/po-separation was not achieved. Synthesis was optimized to crude yields of 76% for pp-; 87% for po-, and 86% for oo-. Subsequently, crosslinked networks were prepared with *meta*-xylylenediamine. With increasing ortho content, degradation of chemical resistance and an inherent weakening of the network was observed, that is, glass transition temperature (T_g), beta transition temperature (T_β), density, crosslink density, and the desorption diffusion coefficient decreased, whereas sorption diffusion coefficient and ultimate solvent uptake increased. This clearly shows that a subtle chemical structure change can significantly impact network performance.



INTRODUCTION

Epoxy resins are used in a wide variety of applications, from coatings to composites. These applications subject the epoxy resin to a wide range of chemical and environmental assailants. Composite structures such as wind turbines and aircraft structures are exposed to weathering, encapsulation coatings may be exposed to challenging chemical environments, high temperatures, or both. This study determines the effect of regioisomerism within diglycidyl ether of bisphenol F (DGEBF) on the chemical performance, in this case the resistance to methanol (selected as a model penetrant), as an indicator of chemical performance, which is an indicator of the barrier this network would form.

Epoxy resin polymer networks are produced on the reaction of multifunctional epoxide molecules with (a) themselves in the presence of a catalyst or (b) another multifunctional reactive component (or “hardener”), such as an anhydride or amine. Bisphenol-based epoxy monomers are commonly used, typically diglycidyl ether of bisphenol A or F (DGEBA or DGEBF). Epoxy networks have a high crosslink density contributing to increased chemical performance and strength/stiffness. These properties can be tuned by adjusting the structure of the network.^{1–3}

Chemical performance describes the resistance of a material to chemical attack—most commonly by solvent, although resistance to oxidation and flammability are also worthy of consideration. Epoxy networks provide good chemical performance and thus protection from a range of solvents as crosslinking means that they are insoluble in any solvent.

However, ingress of solvent molecules into the networks is possible, which causes swelling. This swelling induces stress in the coating and in turn damage—therefore, longevity of the coating is related to the solvent uptake.^{4,5} Furthermore, swelling leads to plasticization, a depression of the glass transition temperature (T_g), and reduced mechanical performance.^{6–10} There are two relevant measures relating to solvent uptake—the amount of uptake and the speed of that uptake. Both the free volume and network polarity (which are both directly related to the network structure) have been identified as important influencing factors for chemical performance.^{9,11–16} To explore the impact that nuanced changes to the network structure have upon chemical performance, it is imperative to produce well-defined networks.

In order to form a well-defined network, ensuring a good extent of reaction between the reactive groups is important. When using hardeners, a key consideration is the ratio of mixing of the reactive components, that is, the stoichiometry. Generally, formulation for the highest crosslink densities involves aiming for a 1:1 (stoichiometric) ratio between reactive sites. In the case of epoxy–amine reactions, this is two epoxy groups per primary amine, as a primary amine can react twice before forming the final tertiary product in the network. The extent of reaction of the reactive groups can be monitored using near-infrared (NIR) spectroscopy.¹⁷

Received: July 10, 2019

Revised: August 9, 2019

The chemical structure of the component parts greatly influences the structure and hence properties of the formed network, such as the glass transition temperature of the network. Two commonly used amines are 3,3'- and 4,4'-diaminodiphenylsulfone—with the difference in their chemical structure being the position of the amine groups around the aromatic rings. Upon stoichiometric cure with DGEBA, they exhibit a 40 °C difference in T_g (4,4' greater than 3,3'), despite this subtle chemical change.¹⁸ Variation in T_g for amines has also been shown using the regioisomers of phenylene diamine.¹⁹

All bisphenol-based epoxy monomers show chain extension: oligomeric forms of the monomer are present in the resin mixture resulting from the synthetic method. Additionally, DGEBF has been shown to contain further complexity in its composition. Nuclear magnetic resonance (NMR) spectroscopy shows that DGEBF contains both *para*- and *ortho*-substitution on the aromatic rings contained within its structure, leading to the presence of the three isomers, *pp*, *po*, and *oo* (Figure 1). Prior to this work, it was not known how this molecular complexity is likely to impact on any subsequent network relative to an individual isomer of DGEBF.

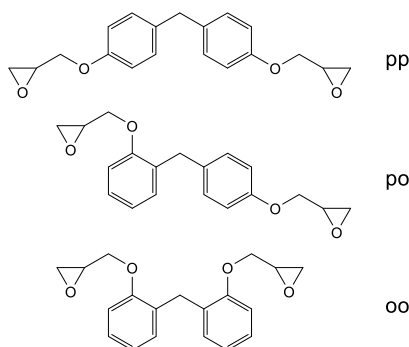


Figure 1. Three isomers of DGEBF, *para*–*para* (ppDGEBF), *para*–*ortho* (poDGEBF), and *ortho*–*ortho* (ooDGEBF).

A wealth of literature exists for the study of the properties and behavior of bisphenol F-based epoxy resins, although discussion of any regioisomerism is in most cases neglected and in some cases the structure is described as a single isomer.^{5,10,16,18,20–23} As these studies use a range of different DGEBF-based resin mixtures and do not discuss the isomeric distribution, there is a risk that changes in properties attributed to another factor may be the result of resins of different compositions. This work seeks to understand the differences between networks consisting of the different regioisomers.

Furthermore, the production of networks with individual isomers will provide insight into the relative impacts of changing geometry and mass between crosslinks in epoxy networks (because they are changed, where polarity remains virtually unchanged). Network properties will be studied using a range of thermal/physical measures (thermal transitions, density, and crosslink density) and solvent uptake as a probe into the free volume and packing of the polymer.

EXPERIMENTAL SECTION

Materials. The following materials were used as supplied: Dow Epoxy Resin 354 (DER 354 (the reaction product of an isomeric mixture of bisphenol F and epichlorohydrin)) (Olin Corporation); bisphenol A, *para*–*para*-bisphenol F, *para*–*ortho*-bisphenol F, and

ortho–*ortho*-bisphenol F (Tokyo Chemical Industry UK Ltd.); epichlorohydrin (Alfa Aesar); crystal violet solution (0.5% solution in glacial acetic acid), *meta*-xylylenediamine (MXDA), and tetrabutylammonium bromide (Sigma-Aldrich Co. Ltd.); tetraethylammonium bromide, acetic acid, and potassium hydroxide (Fisher Scientific); and perchloric acid (0.1 mol L⁻¹ solution in acetic acid) (VWR International).

Preparatory High-Performance Liquid Chromatography. A Varian ProStar high-performance liquid chromatography (HPLC) system was used, with two 210 pumps and a 320 UV detector. The autosampler used was a 410 model, with a 1000 μ L injection loop. The column (19 \times 250 mm) was a Waters XBridge Prep C18 5 μ m OBD. The detector was operated at 280 nm, and the system was run at a flow rate of 17.0 mL min⁻¹.

NMR Spectroscopy. All NMR spectroscopy was completed using a Bruker AVANCE 400 MHz spectrometer. Chemical shifts are given relative to the lock solvent.

Titration for Epoxide Equivalent Weight. Tetraethylammonium bromide (40 g, 0.19 mol) was dried for approx. 1 h at 100 °C. It was then dissolved with warming in acetic acid (450 cm³) and allowed to cool. Eight drops of 0.5% crystal violet solution in acetic acid were added, and the mixture neutralized to an emerald green color using 0.1 mol dm⁻³ perchloric acid in acetic acid (approx. 5 cm³). Samples of DER 354 (approx. 0.1 g) were dissolved in this mixture and then titrated with 0.1 mol dm⁻³ perchloric acid in acetic acid to the emerald green end-point. The epoxide equivalent weight (EEW) was then calculated from eq 1, where m is mass of the sample, T is the titre, and $[PA]$ is the concentration of perchloric acid.

$$EEW = \frac{m}{T \times [PA]} \quad (1)$$

Column Chromatography of DER 354. The low molecular weight components, that is the isomers of diglycidyl ether bisphenol F, present in DER 354 (11 g) were separated by column chromatography, with a column volume of approximately 1400 cm³. The stationary phase was 0.6 Å silica for flash chromatography. The mobile phase was 35:65 ethyl acetate/hexane. Two main fractions were obtained [F_1 (average mass obtained 1.05 g), F_2 (average mass obtained 5.45 g)].

Optimization of Epoxidation of Bisphenol A. Route A: bisphenol A (2.279 g, 9.98 mmol) was dissolved in epichlorohydrin (8 mL) and stirred for 6 h at room temperature. To this, potassium hydroxide (0.7 g, 12.5 mmol) in water (6 mL), pentane (10 mL), and diethyl ether (10 mL) were added. The mixture was stirred for a further 12 h. The organic layer was separated and washed with water and dried over magnesium sulfate. The solvent and epichlorohydrin were removed under vacuum to give a yellowish resin (2.90 g, 8.52 mmol, 85.4%). Route B: ground potassium hydroxide (1.50 g, 26.7 mmol) and tetrabutylammonium bromide (0.32 g, 0.993 mmol) was added with stirring to bisphenol A (2.00 g, 8.76 mmol) dissolved in epichlorohydrin (10 mL). This solution was then stirred overnight. Water was added to the solution, and the organic layer separated. The aqueous layer was extracted with diethyl ether twice and ethyl acetate once. The four organic layers were combined and washed three times with water, before drying over magnesium sulfate. Finally, the solvent and epichlorohydrin were removed under vacuum to give a colorless resin (2.63 g, 7.73 mmol, 89%).

Synthesis of Isomers. Ground potassium hydroxide (approx. 6 g, 108 mmol) and tetrabutylammonium bromide (approx. 1.2 g, 3.62 mmol) were added with stirring to an isomer of bisphenol F (approx. 7 g, 35 mmol) dissolved in epichlorohydrin (40 mL). This solution was then stirred for 3 to 6 days. Water was added to the solution, and the organic layer separated. The aqueous layer was extracted with diethyl ether once and ethyl acetate twice. The four organic layers were combined and washed three times with water, before drying over magnesium sulfate. Finally, the solvent and epichlorohydrin were removed under vacuum to give crude product (average yields 93, 87, and 86% for *pp*, *po*, and *oo*, respectively). The *po*- and *oo*-DGEBF products required column chromatography (see below for details) to be performed to obtain a product of good purity. The *pp*-DGEBF was

an off-white waxy solid ($^1\text{H NMR}$ (C_6D_6 , 400 MHz): δ 2.13 (dd, 1H, $J = 5.2, 2.4$ Hz), 2.25 (dd, 1H, $J = 5.2, 4.0$ Hz), 2.86–2.92 (m, 1H), 3.45 (dd, 1H, $J = 11.2, 5.6$ Hz), 3.65 (dd, 1H, $J = 11.2, 3.2$ Hz), 3.74 (s, 1H), 6.76–6.81 (m, 2H), and 6.95–7.04 (m, 2H)), residual internal $\text{C}_6\text{D}_5\text{H}$, the poDGEBF was a yellowish liquid, which slowly solidified to an off-white waxy solid, and ooDGEBF was a white solid.

Column Chromatography of Crude po- and oo-DGEBF of Isomers. Crude poDGEBF/ooDGEBF was purified by a standard column chromatography procedure with a column volume of approximately 1400 cm^3 . The stationary phase was 40–63 μm silica for flash chromatography. The mobile phase was 35:65 ethyl acetate/hexane. The total poDGEBF obtained was 10.9290 g (35.0 mmol, total yield: 62%) ($^1\text{H NMR}$ (C_6D_6 , 400 MHz): δ 2.11–2.18 (m, 2H), 2.23–2.29 (m, 2H), 2.82–2.91 (m, 2H), 3.39–3.49 (m, 2H), 3.61–3.67 (m, 2H), 4.00 (s, 2H), 6.54 (d, 1H, $J = 8.4$ Hz) 6.76–6.82 (m, 2H), 6.84–6.89 (m, 1H), 7.03–7.10 (m, 2H), and 7.12–7.18 (m, overlap with residual solvent), and ooDGEBF obtained was 10.6628 g (34.1 mmol, total yield: 52%) ($^1\text{H NMR}$ (C_6D_6 , 400 MHz): δ 2.14 (dd, 1H, $J = 5.2, 2.4$ Hz), 2.25 (dd, 1H, $J = 5.2, 4.0$ Hz), 2.83–2.88 (m, 1H), 3.45 (ddd, 1H, $J = 11.2, 5.6, 2.0$ Hz), 3.65 (dd, 1H, $J = 11.2, 3.2$ Hz), 4.26 (s, 1H), 6.56 (d, 1H, $J = 8.0$ Hz), 6.87 (t, 1H, $J = 7.4$ Hz), 7.06 (td, 1H, $J = 11.1, 4.0$ Hz), and 7.23 (dd, 1H, $J = 7.2, 1.2$ Hz).

Glass Slide Preparation. Hydrogen peroxide was added with care and gentle stirring to sulfuric acid in a 1:3 ratio to produce the “piranha solution”. Slides (as supplied) were placed in the “piranha solution” and left for 15 min before rinsing thoroughly with deionized water. The treated slides were placed in a rack and dried at $50\text{ }^\circ\text{C}$ in an oven and stored there until use.

NIR Spectroscopy. NIR spectroscopy was performed on an Ocean Optics NIRQuest 2500. Spectra were sampled using an integration time of 10 ms and taking 100 scans to average. Sample cells were prepared using a PTFE spacer between glass slides, fastened together using a small amount of epoxy resin. For the molar extinction coefficient determination with varied path length, different thicknesses (approx. 0.55, 0.6, 0.8, 0.85 mm) of PTFE were used to make the cells. For degree of cure measurements, cells with a path length of 0.55–0.6 mm were used, and cure completed in a heated cell, using the same cure schedule as that described in the subsequent section. Spectra were obtained throughout the cure.

Network Preparation for Solvent Sorption/Desorption Studies. Formulation (DER 354). DER 354 was added to MXDA in a 1:1 stoichiometric ratio of epoxide to amine functional groups, and then mixed by hand, using a stirring rod. The resulting mixture was covered using a parafilm (to limit any interaction with oxygen or carbon dioxide or evaporation of the amine) and held, with further mixing (initially every 5 min, then less regularly), at room temperature. After 180 min, the mixture was applied to glass slides (see below).

Formulation (po/ppDGEBF). Epoxy resin was added to MXDA in a 1:1 stoichiometric ratio of epoxide to amine functional groups and then mixed by hand, using a stirring rod. The resulting mixture was covered using a parafilm (to limit any interaction with oxygen or carbon dioxide or evaporation of the amine) and held, with further mixing (initially every 5 min, then less regularly), at $33\text{ }^\circ\text{C}$ (to prevent recrystallization). Upon any clouding, indicating recrystallization, the mixture was heated with a heat gun until melted—and then returned immediately to $33\text{ }^\circ\text{C}$. After 75 min, the mixture was applied to glass slides (see below).

Formulation (ooDGEBF). ooDGEBF was added to MXDA in a 1:1 stoichiometric ratio of epoxide to amine functional groups and then mixed by hand, using a stirring rod. The resulting mixture was covered using parafilm and held, with further mixing (initially every 5 min, then less regularly), at a higher temperature of $40\text{ }^\circ\text{C}$ (here, recrystallization presented a much greater issue). Upon excessive clouding, the mixture was heated with a heat gun followed by immediate cooling back to $40\text{ }^\circ\text{C}$. After 20 min, the mixture was applied to glass slides (see below).

Application to Slides. The mixtures described above were drawn-down onto prepared glass slides held at $30\text{ }^\circ\text{C}$, using a 400 μm slit,

drawdown cube (Sheen Instruments). The slides were then placed in an oven and cured under a nitrogen atmosphere. Oxygen-free nitrogen, obtained from BOC, was purged through the oven at approx. $5\text{ cm}^3\text{ min}^{-1}$. The cure schedule was an initial temperature of $60\text{ }^\circ\text{C}$, with a ramp of $1\text{ }^\circ\text{C min}^{-1}$ to $160\text{ }^\circ\text{C}$, where the oven was held for 3 h. Upon completion of the 3 h, the samples were removed from the oven and allowed to cool from $160\text{ }^\circ\text{C}$. All samples were uniform, colorless, and clear films. Any samples not immediately analyzed were placed in a desiccator over phosphorus pentoxide to prevent moisture uptake.

Dynamic Mechanical Analysis. Dynamic mechanical analysis (DMA) was performed on a PerkinElmer DMA8000, using the single cantilever mode, heated at a rate of $3\text{ }^\circ\text{C min}^{-1}$. Three beams were prepared for each sample formulation, approximately 10 mm wide and 1.6 mm thick, and the dynamic response to a sinusoidal force applied at a frequency of 1 s^{-1} was recorded. The T_g was taken as the temperature at the highest intensity of the peak in the $\tan\delta$ trace from a Lorentzian fit of the peak using OriginLab 2017. For the β -transition measurements, the sample chamber was cooled to approximately $-192\text{ }^\circ\text{C}$, before the measurement was performed. The area of the peak was obtained using a fitted cubic baseline and integrating the area beneath the curve. Crosslink density, ν , is calculated from eq 2, where E is the rubbery plateau storage modulus (taken as the storage modulus at $T_g + 40\text{ K}$), R is the gas constant, and T is temperature.²⁴

$$\nu = \frac{E}{3RT} \quad (2)$$

Helium Pycnometry. Helium pycnometry was performed on a Micrometrics AccuPyc 1330, using approximately 0.4 g of sample in a sample cell of 1 cm^3 and a standard of known mass and volume for calibration.

Methanol Sorption/Desorption Measurements. Coated glass slides were placed in methanol, upright and separate using Coplin jars, and weighed at time intervals ranging from 16 h to 90 days (see the Supporting Information). Intervals between measurements were increased as time increased due to the slowing of mass uptake. Upon reaching a plateau in mass, these samples were removed from the solvent and placed in an oven at $40\text{ }^\circ\text{C}$, and weighed at time intervals until a reasonable plateau was obtained (a return to the original dry mass was only possible upon heating to $120\text{ }^\circ\text{C}$ under reduced pressure).

RESULTS AND DISCUSSION

In approaching an isolated epoxy resin isomer, there are two main approaches: (a) separate from an industrially available mixture of the isomers or (b) synthesize from individual pure starting materials. First, separation from DER 354 was considered. NMR spectroscopy shows DER 354 consists of a 3.5:3.2:1 pp/po/oo ratio, determined as per the method described by Domke.²⁵ This is not however the ratio of the three simplest molecules, rather the ratio of the substitution. The oligomeric structures (e.g., Figure 2) in the resin mixture also contribute to this ratio. If we consider the ways in which the original three structures can combine (regioisomeric motifs), when considering our reactant on a molecular level, we can say that there are at least 12 different “monomers” from which the network is built if $n \leq 1$.

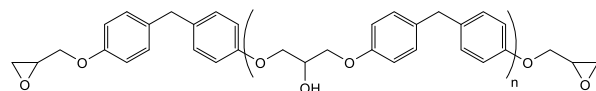


Figure 2. An example of a chain-extended oligomer of DGEBF, while only considering para-substitution. Each phenylene ring can be either ortho- or para-substituted when considering the diversity of possible isomers for a particular degree of chain extension (i.e., value of n).

Ponten showed that HPLC can be used to separate the isomers of DGEGBF.²⁶ With an adjusted method, we have also attained separation. Figure 3 shows the initial analytical HPLC

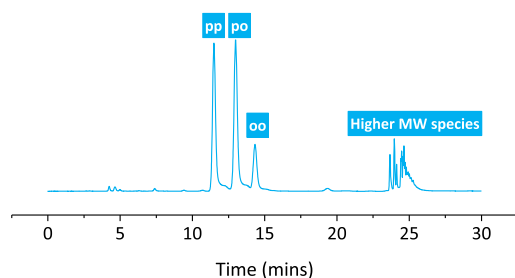


Figure 3. HPLC chromatogram for DER 354 using a 50:50 acetonitrile/water isocratic solvent system. The major peaks are labeled with the responsible component of a DGEGBF-based mixture. The region at 23–36 min illustrates the large number of different higher molecular weight “monomers”.

data, showing three pronounced peaks at 10–15 min and a more complex region at 25 min. Preparatory HPLC yielded samples of the three monomeric forms confirmed by NMR spectroscopy. The region at 23–26 min illustrates the number of different oligomeric species present. The number of distinct peaks shows the number of different oligomeric species present. Despite successful separation, the cost is very high with only milligram quantities isolated and HPLC is therefore unsuitable for network preparation.

A more widely used chromatographic method is column chromatography. Thin layer chromatography showed separation between two main spots, with one being much bolder than the other (R_f values of 0.42 and 0.49, respectively). The faster eluting compound (fainter spot) was isolated by column chromatography and found to be the oo isomer. The major spot was shown to be a mixture of the pp and po isomers. Within this eluted fraction, it was shown that initially the fraction was richer in po, becoming richer in pp in progressing through the fraction. Both NMR spectroscopy and titration to obtain EEW (the mass per mole of epoxide groups) show that the higher oligomers have been removed. The quantities isolated were larger, with the column scaled to allow loading of approx. 11 g of DER354. However, because of the small proportion of ooDGEGBF in DER 354, less than 2 g was isolated per column. Hence, chromatographic methods offer an expensive route to very high purity isomers (HPLC) or a simpler route to a partly purified reactant mixture (column).

As the chromatographic approach did not yield an effective route to individual pp and po, the synthetic route was considered. Rather costly individual isomers of bisphenol F were available from TCIUK. Therefore, in order to ensure that the reaction was efficient and high-yielding, an optimization of the synthetic route was performed using bisphenol A. The two routes identified from the literature differ in the nature of the reaction mixture—route A, from Wengert et al., involving a biphasic aqueous/organic mixture stirred vigorously, and route B from Zhou et al. was an organic/solid mixture.^{27,28}

Following synthesis, the quality of the product was analyzed by NMR spectroscopy. Route A showed problems with incomplete conversion, unwanted side-products, and chain extension. However, route B was shown to be much more efficient. This process was then optimized for the ratio of reactants, adjusting both TBAB and PTC concentrations. It is

difficult to eliminate all chain extension, but as the starting material only contains the single regioisomer, the number of possible molecules is substantially reduced (from 12 to 2). Route B was shown to produce the epoxide molecule in an 89% yield, in a good degree of purity.

This method was then applied to the individual bisphenol F isomers, with crude yields of 76, 87, and 86% for pp-, po-, and oo-DGEGBF, respectively. NMR spectroscopy showed the spectra in general agreement with the targeted products (with some disparities in the oo-, especially in the aromatic region). The HPLC trace of ppDGEGBF shows a single isomer in the monomeric region and, as expected, a substantially simpler oligomeric region, with only a single regioisomeric motif within the molecules (i.e., pp–pp/pp–pp–pp rather than pp–po or pp–po–op). Titration for EEW showed some chain extension, but lower than DER 354, with an average n of 0.05. Similar results were obtained for the po isomer—the increased diversity in the oligomeric region is due to different modes of addition of two po units (po–op/op–op/op–po). However, the EEW was found to be 170.6 g mol^{-1} —corresponding to an n of 0.11. Furthermore, the obtained ooDGEGBF showed an unexpectedly diverse oligomeric region in the HPLC chromatogram and an even higher EEW (181.6 g mol^{-1} — $n = 0.20$). In order to produce comparable networks, column chromatography was performed on both the oo and po isomers.

Column chromatography gave much purer compounds for both of the isomers. Using a mobile phase of 45:55 ethyl acetate/*n*-hexane, quantities above 10 g were obtained (Table 1). The variation in total yield shows the relative impurity of

Table 1. Yields of oo- and po-DGEGBF Obtained from Column Chromatography Over Two Runs of Approximately Equal Loadings per Isomer

	mass loaded/g	mass obtained/g
ooDGEGBF	21.62	12.89 (60%)
poDGEGBF	15.24	10.93 (72%)

the crude ooDGEGBF, as expected from the HPLC and NMR data. For the purified products, n was found to be 0.04 for the po and 0.07 for the oo. Furthermore, the HPLC and NMR data showed good agreement with expected spectra—with significantly reduced complexity in the higher MW region. The ^1H NMR spectra and HPLC chromatograms of the final products are shown in the Supporting Information—Figures S1 & S2.

In order to compare the performance of the various isomers, they were cured in a stoichiometric ratio with MXDA. The industrial DGEGBF-based resin, DER 354 was also cured using the same hardener and method to provide a comparison. Degree of cure measured by NIR spectroscopy showed complete or near-complete reaction for all samples: 100.0% for the pp, po, and DER 354 and 97.3% for the oo (this slight reduction for the oo network, however, as our forthcoming publication shows, has little impact on network properties) and therefore the key factor in any observed property change will be driven by the chemistry changes. It is worth noting that further to the evidence given by NIR spectroscopy, the curing networks were held for 3 h at 160°C , well above the ultimate T_g for each of the networks (ultimate T_g s are between 107 and 117°C —as shown in Figure 4), supporting that complete/near-complete reaction has been achieved.

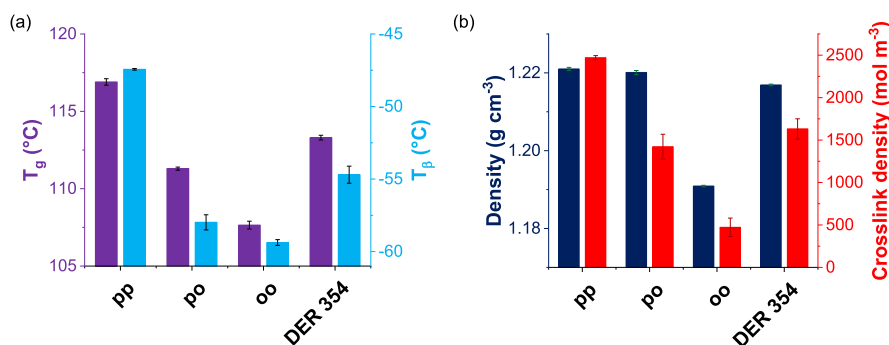


Figure 4. Physical properties of networks produced using MXDA as the amine monomer and *para-para-* (pp), *para-ortho-* (po), and *ortho-ortho-* (oo)-DGEGBF or Dow Epoxy Resin 354 (DER 354) as the epoxide monomer. (a) Glass transition temperature (T_g), the β -transition temperature (T_β) as determined by DMA and (b) crosslink density as determined by DMA (calculated from eq 2—see Experimental Section) and density as determined by helium pycnometry. Error bars show standard error for three samples for T_g and crosslink density, standard error for two samples for T_β and standard deviation of ten measurements of a single sample for density.

Networks produced with the isolated isomers and DER 354 show clear differences in thermal/physical properties. Figure 4 shows the glass transition temperature (T_g), beta-transition temperature (T_β), bulk density, and crosslink density for the networks. Considering the isomers in isolation, decreases in T_g , T_β , density (only for oo), and crosslink density are observed as the ortho-content increases. As might be expected, for a mixture of isomers, DER 354 shows intermediate properties for T_g , T_β , density, and crosslink density, relative to the two extremes represented by pp and oo. Generally, the results indicate the production of a better packed network as the ortho-content is decreased. β -Transition measurements are indicative that there is a molecular motion present for the pp and po networks that is significantly reduced for the oo—shown by a much-reduced peak area for the oo network (Figure 5). This may facilitate the enhanced packing (higher

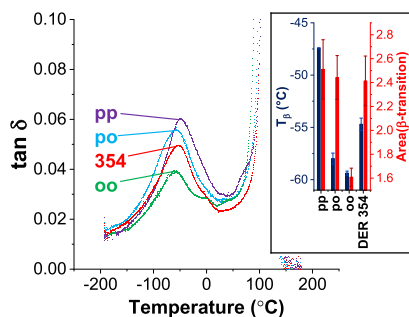


Figure 5. DMA measurement of $\tan \delta$ vs temperature, showing the β -transition for the networks produced using MXDA as the amine monomer and *para-para-* (pp), *para-ortho-* (po), and *ortho-ortho-* (oo)-DGEGBF or Dow Epoxy Resin 354 (DER 354) as the epoxide monomer. Inset: the T_β and area of the peak associated with the β -transition for each of the networks. Error bars show standard error of two samples.

density) that is achieved for these networks. The beta transition for DER 354 appears to be a convolution of the three isomerically pure networks, both in terms of temperature and shape (particularly the shoulder observed in the oo trace at approx. -10 °C).

The networks produced were also shown to vary with respect to their chemical performance—results from methanol sorption are shown in Figure 6. The pp network was shown to uptake the least amount of methanol, at the slowest rate

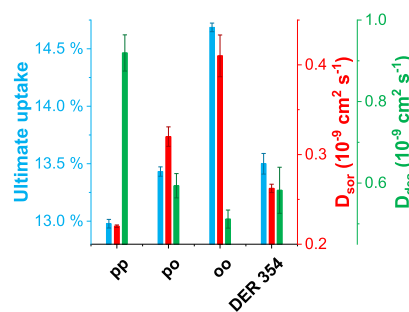


Figure 6. Chemical performance in methanol of networks produced using MXDA as the amine monomer and *para-para-* (pp), *para-ortho-* (po), and *ortho-ortho-* (oo)-DGEGBF or Dow Epoxy Resin 354 (DER 354) as the epoxide monomer. Shown are the ultimate uptake (by original mass) of each network and the diffusion coefficients of sorption (D_{sor}) and desorption (D_{des} , at 40 °C). Error bars show standard error of the three samples.

(quantified by the sorption diffusion coefficient, D_{sor}), and it had the highest value for the desorption diffusion coefficient (D_{des}). The oo network had by far the highest uptake and D_{sor} and the lowest D_{des} . As with thermal/physical properties, the po network showed intermediate properties relative to the other two regioisomers. Similarly, the industrial mixture, DER 354, showed intermediate properties. When the chemical performance is considered alongside the thermal/physical properties, there is strong evidence that regioisomerism leads to a significant shift in network structure and performance. This is not to suggest any knowledge of longer-range structure, rather that the change in molecular structure of the monomer gives rise to notable differences between the networks formed and therefore an inherent difference in the molecular structure of the respective networks.

The combined measurements suggest that the effectiveness of network packing is influenced by the amount of ortho-/para-substitution. They suggest that a well-packed network is formed by ppDGEGBF—because it has the highest density and crosslink density and lowest ultimate uptake. By contrast, the properties obtained for the ooDGEGBF network suggest that the ortho moieties inhibit packing with a much-reduced density and increased ultimate uptake. The reduction in properties for the po network relative to the pp is supportive of the view that ortho-substitution is inhibitive to packing. Although it is not strongly correlated with the density measurement, an increase

in ultimate uptake suggests greater free volume and a reduced crosslink density.

Considering the DER 354, which has an ortho-content of 0.375, as has already been discussed, there is similarity with the po in the observed properties—crosslink density, ultimate uptake, and D_{des} measurements are similar within error, and the variation in density is limited. Generally, these results further support the finding that ortho-substitution is a major influence in network performance (and therefore structure), although the disparity in the ortho-content between po and DER 354 does also show that other factors will impact upon these properties. For example, the degree of chain extension in DER 354 is much higher than for the purer networks.

Figure 7 shows the varied methanol sorption profiles of the three isomers—what is immediately clear is the sigmoidal

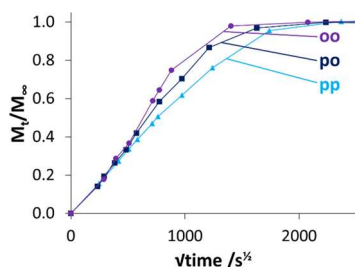


Figure 7. Methanol sorption profiles of DGEGBF/MXDA networks made with the different isomers of DGEGBF [para–para- (pp), para–ortho- (po), and ortho–ortho (oo)]. The individual data points are shown joined with straight lines.

nature of the uptake for the po and oo isomers relative to the Fickian ppDGEGBF. This mode is attributed to swelling processes, which the oo network is most susceptible to (as it has the largest change in gradient).²⁹

CONCLUSIONS

This work shows a significant variation between the properties of networks made with different regioisomers of DGEGBF. Networks of MXDA and DER 354, an industrial mixture of the three regioisomeric structures (in addition to some chain extension) showed intermediate properties relative to networks created with the three isomers. There is a clear improvement in chemical performance with increased para-substitution (vs ortho-substitution). Although processability and practicality may mean that an individual isomer is not a sensible choice for widescale application, the relative proportions of these regioisomers are likely to impact upon the properties of the coatings obtained. These findings emphasize the importance of chemical analysis of bisphenol F-based resins prior to use in other comparisons, so that any property changes might be understood in the light of the isomeric ratio.

ASSOCIATED CONTENT

Supporting Information

The Supporting Information is available free of charge on the ACS Publications website at DOI: 10.1021/acs.macromol.9b01441.

Structural analysis of synthesized monomers; assigned NMR spectra and HPLC chromatograms for the synthesized pp, po, and oo isomers; example weighing schedule for methanol sorption; evolution of NIR spectra over time of a reacting mixture of ppDGEGBF

and MXDA at 160 °C; and details of conversion calculation from NIR spectroscopy (PDF)

AUTHOR INFORMATION

Corresponding Author

*E-mail: s.knox@leeds.ac.uk.

ORCID

Stephen T. Knox: 0000-0001-5276-0085

John Patrick Anthony Fairclough: 0000-0002-1675-5219

Present Address

[§]School of Chemical and Process Engineering, University of Leeds, Leeds, LS2 9JT.

Author Contributions

The manuscript was written through contributions of all authors. All authors have given approval to the final version of the manuscript.

Funding

Funding for S.T.K. from EP/L016281/1 EPSRC Centre for Doctoral Training in Polymers, Soft Matter and Colloids.

Notes

The authors declare no competing financial interest.

ACKNOWLEDGMENTS

The authors would like to thank AkzoNobel and the EPSRC for funding via the CDT in Polymers, Soft Matter and Colloids; and Dr. Joel Foreman and Roderick Ramsdale-Capper for DMA access.

REFERENCES

- (1) LeMay, J. D.; Kelley, F. N. Structure and Ultimate Properties of Epoxy Resins. In *Epoxy Resins and Composites III SE—4*; Dušek, K., Ed.; Advances in Polymer Science; Springer Berlin Heidelberg, 1986; Vol. 78, pp 115–148.
- (2) Pascault, J. P.; Sautereau, H.; Verdu, J.; Williams, R. J. J. *Thermosetting Polymers; Plastics Engineering*; Taylor & Francis: New York, 2002.
- (3) Cameron, C.; Port, A. B. P. Film Formation. In *The Chemistry and Physics of Coatings*; Marrion, A., Ed.; The Royal Society of Chemistry: Cambridge, 2004; pp 46–63.
- (4) Frank, K.; Childers, C.; Dutta, D.; Gidley, D.; Jackson, M.; Ward, S.; Maskell, R.; Wiggins, J. Fluid Uptake Behavior of Multifunctional Epoxy Blends. *Polymer* **2013**, *54*, 403–410.
- (5) Alessi, S.; Toscano, A.; Pitarresi, G.; Dispenza, C.; Spadaro, G. Water Diffusion and Swelling Stresses in Ionizing Radiation Cured Epoxy Matrices. *Polym. Degrad. Stab.* **2017**, *144*, 137–145.
- (6) Weitsman, Y. J.; Guo, Y.-J. A Correlation between Fluid-Induced Damage and Anomalous Fluid Sorption in Polymeric Composites. *Compos. Sci. Technol.* **2002**, *62*, 889–908.
- (7) Nogueira, P.; Ramirez, C.; Torres, A.; Abad, M. J.; Cano, J.; Lopez, J.; Lopez-Bueno, I.; Barral, L. Effect of Water Sorption on the Structure and Mechanical Properties of an Epoxy Resin System. *J. Appl. Polym. Sci.* **2001**, *80*, 71–80.
- (8) Theocaris, P. S.; Kontou, E. A.; Papanicolaou, G. C. The Effect of Moisture Absorption on the Thermomechanical Properties of Particulates. *Colloid Polym. Sci.* **1983**, *261*, 394–403.
- (9) Jackson, M.; Kaushik, M.; Nazarenko, S.; Ward, S.; Maskell, R.; Wiggins, J. Effect of Free Volume Hole-Size on Fluid Ingress of Glassy Epoxy Networks. *Polymer* **2011**, *52*, 4528–4535.
- (10) Pitarresi, G.; Toscano, A.; Alessi, S. Fracture Toughness of Synthesised High-Performance Epoxies Subject to Accelerated Water Aging. *Polym. Test.* **2018**, *68*, 248.
- (11) Port, A. B.; Cameron, C. Performance Properties of Coatings. In *The Chemistry and Physics of Coatings*; Marrion, A., Ed.; Royal Society of Chemistry: Cambridge, 2004; pp 64–95.

- (12) Zhang, S.-Y.; Ding, Y.-F.; Li, S.-J.; Luo, X.-W.; Zhou, W.-F. Effect of Polymeric Structure on the Corrosion Protection of Epoxy Coatings. *Corros. Sci.* **2002**, *44*, 861–869.
- (13) Soles, C. L.; Chang, F. T.; Bolan, B. A.; Hristov, H. A.; Gidley, D. W.; Yee, A. F. Contributions of the Nanovoid Structure to the Moisture Absorption Properties of Epoxy Resins. *J. Polym. Sci., Part B: Polym. Phys.* **1998**, *36*, 3035–3048.
- (14) Soles, C. L.; Yee, A. F. A Discussion of the Molecular Mechanisms of Moisture Transport in Epoxy Resins. *J. Polym. Sci., Part B: Polym. Phys.* **2000**, *38*, 792–802.
- (15) Soles, C. L.; Chang, F. T.; Gidley, D. W.; Yee, A. F. Contributions of the Nanovoid Structure to the Kinetics of Moisture Transport in Epoxy Resins. *J. Polym. Sci., Part B: Polym. Phys.* **2000**, *38*, 776–791.
- (16) Toscano, A.; Pitarresi, G.; Scafidi, M.; Di Filippo, M.; Spadaro, G.; Alessi, S. Water Diffusion and Swelling Stresses in Highly Crosslinked Epoxy Matrices. *Polym. Degrad. Stab.* **2016**, *133*, 255–263.
- (17) Mijovic, J.; Andjelic, S. A Study of Reaction Kinetics by Near-Infrared Spectroscopy. I. Comprehensive Analysis of a Model Epoxy/Amine System. *Macromolecules* **1995**, *28*, 2787–2796.
- (18) Frank, K.; Wiggins, J. Effect of Stoichiometry and Cure Prescription on Fluid Ingress in Epoxy Networks. *J. Appl. Polym. Sci.* **2013**, *130*, 264–276.
- (19) Riad, K. B.; Schmidt, R.; Arnold, A. A.; Wuthrich, R.; Wood-Adams, P. M. Characterizing the Structural Formation of Epoxy-Amine Networks: The Effect of Monomer Geometry. *Polymer* **2016**, *104*, 83–90.
- (20) Kravchenko, O. G.; Li, C.; Strachan, A.; Kravchenko, S. G.; Pipes, R. B. Prediction of the Chemical and Thermal Shrinkage in a Thermoset Polymer. *Composites, Part A* **2014**, *66*, 35–43.
- (21) Oya, Y.; Kikugawa, G.; Okabe, T. Clustering Approach for Multidisciplinary Optimum Design of Cross-Linked Polymer. *Macromol. Theory Simul.* **2017**, *26*, 1600072.
- (22) Lange, J.; Altmann, N.; Kelly, C. T.; Halley, P. J. Understanding Vitrification during Cure of Epoxy Resins Using Dynamic Scanning Calorimetry and Rheological Techniques. *Polymer* **2000**, *41*, 5949–5955.
- (23) Childers, C. H.; Hassan, M. K.; Mauritz, K. A.; Wiggins, J. S. Molecular Scale Cure Rate Dependence of Thermoset Matrix Polymers. *Arabian J. Chem.* **2016**, *9*, 206–218.
- (24) Treloar, L. R. G. *The Physics of Rubber Elasticity*; Treloar, L. R. G., Ed.; Oxford University Press: Oxford, United Kingdom, 2005.
- (25) Domke, W.-D. ¹H NMR Spectroscopic Determination of the Isomeric Ratios of Bisphenol-F Diglycidyl Ethers. *Org. Magn. Reson.* **1982**, *18*, 193–196.
- (26) Ponten, A.; Zimerson, E.; Sorensen, O.; Bruze, M. Chemical Analysis of Monomers in Epoxy Resins Based on Bisphenols F and A. *Contact Dermatitis* **2004**, *50*, 289–297.
- (27) Wengert, M.; Sanseverino, A. M.; Mattos, M. C. S. d. Trichloroisocyanuric Acid: An Alternate Green Route for the Transformation of Alkenes into Epoxides. *J. Braz. Chem. Soc.* **2002**, *13*, 700–703.
- (28) Zhou, Y.; Jiang, C.; Zhang, Y.; Liang, Z.; Liu, W.; Wang, L.; Luo, C.; Zhong, T.; Sun, Y.; Zhao, L.; et al. Structural Optimization and Biological Evaluation of Substituted Bisphenol A Derivatives as Beta-Amyloid Peptide Aggregation Inhibitors. *J. Med. Chem.* **2010**, *53*, 5449–5466.
- (29) De Kee, D.; Liu, Q.; Hinestroza, J. Viscoelastic (Non-Fickian) Diffusion. *Can. J. Chem. Eng.* **2008**, *83*, 913–929.